

Bis[(3,5-dimethyl-1-pyrazolyl)methyl]ethylamine – A Versatile Ligand for Complexation in Rh^I Cationic Complexes

René Mathieu,^{*[a]} Glòria Esquiús,^[a,b] Noël Lugan,^[a] Josefina Pons,^[b] and Josep Ros^{*[b]}

Keywords: Rhodium / Aminopyrazole / Hemilabile ligands / Cationic complexes

The bis[(3,5-dimethyl-1-pyrazolyl)methyl]ethylamine ligand (**1**) reacts with [Rh(COD)(THF)₂][BF₄] leading to [Rh(COD)(**1**)](BF₄) (**[2]**[BF₄]) in which **1** is κ^3 bonded in the solid state. Because of the steric bulk of 1,5-cyclooctadiene, it prefers the κ^2 mode of bonding in solution. Substitution of 1,5-cyclooctadiene by carbon monoxide generates **[3]**[BF₄] in which **1** is κ^3 bonded in solution and solid state. Variable tem-

perature NMR spectroscopic studies give evidence of a $\kappa^3 \rightleftharpoons \kappa^2$ equilibrium in solution. **[3]**[BF₄] is easily decarbonylated to [Rh(CO)(**1**)](BF₄) (**[4]**[BF₄]) in which **1** is κ^3 bonded; however on bubbling carbon monoxide through, **[3]**[BF₄] is regenerated. The single-crystal X-ray structures of **[2]**[BF₄], **[3]**[BPh₄], and **[4]**[BPh₄] are reported.

Introduction

The readily available pyrazolyl group has allowed the construction of various bi- or polydentate ligands, thus furnishing metal complexes of varying coordination geometry and nuclearity.^[1–4] One of the reasons for this success arises from the ability to change the nature, number, and position of substituents in the pyrazole ring, thus allowing a fine tuning of the reactivity of the metal centre to which they are bound. For instance, the most well-developed ligands, the poly(pyrazolyl)borates and their complexes, have found interesting applications in catalysis and bioinorganic chemistry.^[1,5–8]

The bonding properties of another family of pyrazole-based chelating ligands, the pyrazole derivatives of simple amines, are also well documented.^[4,9,10] They are considered to be hard donor ligands, and the studies of their bonding properties have focussed on cations in high oxidation states, essentially to provide routes to a variety of bioinorganic model systems, or to evaluate their extracting properties. Prompted by the increasing success in catalysis of complexes containing amino ligands,^[11–13] it was thought interesting to probe the bonding properties of aminopyrazoles toward soft cations, such as Rh^I. In contrast to the well studied tris(pyrazolyl)borate/Rh^I systems,^[14–16] these ligands contain two types of donating centres with different degrees of hardness which might be expected to exhibit different types of behaviour toward the soft Rh^I centre.

We here describe the interactions of a typical aminopyrazole, bis[(3,5-dimethyl-1-pyrazolyl)methyl]ethylamine (**1**) towards a series of cationic Rh^I complexes.

Results and Discussion

Bis[(3,5-dimethyl-1-pyrazolyl)methyl]ethylamine (**1**) reacts with [Rh(COD)(THF)₂][BF₄] – generated in situ from the reaction of [Rh(COD)Cl]₂ and AgBF₄ in THF – to give the complex [Rh(COD)(**1**)](BF₄) (**[2]**[BF₄]) in 90% yield. At room temperature, the proton NMR spectrum of **[2]**⁺ shows the presence of two isomers **[2a]**⁺ and **[2b]**⁺ in a 2:1 ratio. The most salient feature of the spectra, and the most significant for probing structural differences, is provided by the N^{Et} resonances, where the ethyl group resonances of the minor isomer are more deshielded than those of **[2a]**⁺. This observation suggests that in **[2b]**⁺ the nitrogen of the amine group is bonded to rhodium, and that the two isomers differ in their coordination to rhodium, which can be either the κ^2 or κ^3 type.

To clarify this point, **[2]**[BF₄] was structurally characterised by X-ray crystallography. The complex crystallises with three independent ion pairs per unit cell. The three cations of **[2]**⁺ present the same geometry, with the respective distances and angles being equal within experimental errors. A view of one of the three independent cations (cation A) appears as Figure 1; selected bond length and angle data are provided in Table 1. In the solid state, only isomer **[2b]**⁺ is observed. The nitrogen of the amino group N3 is 2.513(7) Å from Rh1; it is longer than the other two Rh–N distances but smaller than the sum of van der Waals radii (3.4 Å). The pyrazolyl-nitrogen to Rh distances are slightly different but are in the range found for hydridotris(pyrazolyl)borate rhodium complexes.^[15,16] The N4–Rh1 bond is significantly longer than the N1–Rh1 bond, and this is certainly the consequence of the steric crowding around rhodium as there are no electronic reasons to justify this differ-

^[a] Laboratoire de Chimie de Coordination du CNRS, 205 Route de Narbonne, 31077 Toulouse Cedex4, France
Fax: (internat.) +30–5 61 55 30 03
E-mail: mathieu@lcc-toulouse.fr

^[b] Departament de Química, Universitat Autònoma de Barcelona, 08193 Bellaterra, Cerdanyola, Spain
Fax: (internat.) +34–93/58 13 101
E-mail: josep.ros@uab.es

ence. This is evident if we consider the positioning of the 1,5-cyclooctadiene ligand. The atoms C15, C18, N1, and N4 lie in a plane, which is usually^[16] defined by the pyrazolyl nitrogen atoms and the middle of the olefinic carbon-carbon bonds. The rhodium atom lies 0.1 Å out of that coordination plane. The position of the cyclooctadiene undoubtedly results from steric crowding attributable to the amino group. Indeed C7 is nearer to C18 carbon than to C15, and lengthening of the Rh1–N4 distance minimises the steric crowding of the ethyl group. Likewise, the C18–Rh1–N4 angle is 10° wider than that of the C15–Rh1–N1 angle. If we consider the pyrazolyl planes, the angle between the mean plane defined by the N4 pyrazolyl ring and the Rh–N4 vector is more acute (142.8°) than the angle between the Rh–N1 vector and the mean plane of the N1 pyrazolyl ring (163.9°). Because of the strain induced by the methylene bridges, the N1–Rh1–N3 and N4–Rh1–N3 angles are around 73°.

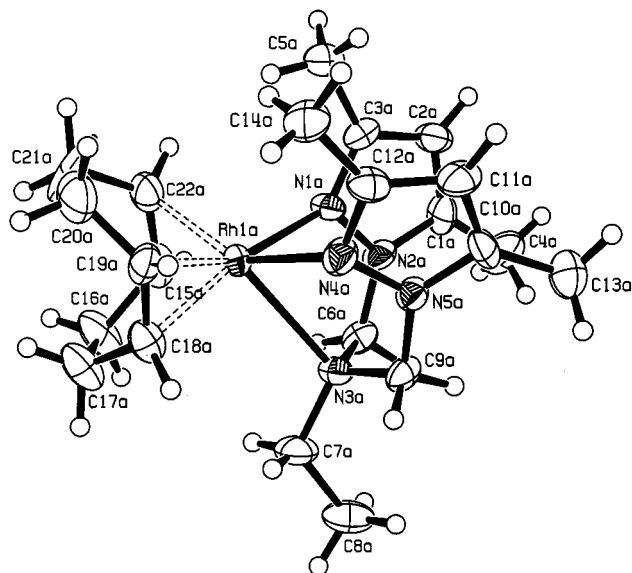


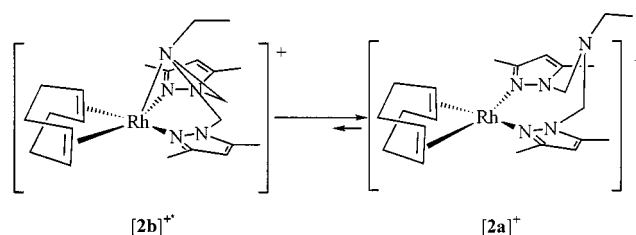
Figure 1. Structure of the cation $[2]^+$ showing the numbering scheme; ellipsoids are drawn at the 50% probability level

To check whether the solid-state structure is maintained in solution, some crystals were dissolved in deuterated dichloromethane at -70°C , and the solution was examined by ^1H NMR spectroscopy at this temperature. Initially, $[2b]^+$ is the major component, but the concentration of $[2a]^+$ slowly increases. When the temperature is raised to 20°C , the previously observed 2:1 ratio of the isomers $[2a]^+/[2b]^+$ is rapidly restored, demonstrating the operation of a thermodynamic equilibrium which favours the less sterically encumbered isomer $[2a]^+$, as summarised in Scheme 1.

We note that, as previously observed by several of the present authors, the reaction of **1** with $[\text{Rh}(\text{COD})\text{Cl}]_2$ leads to $[\text{Rh}(\text{COD})(\mathbf{1})]^+[\text{Rh}(\text{COD})\text{Cl}_2]^-$.^[17] However, in contrast to $[2]^+$, the cationic part of this latter complex is characterised by broad ^1H NMR peaks assignable to ligand **1**, supporting the author's earlier hypothesis concerning the existence of an equilibrium in solution between the ionic

Table 1. Selected bond lengths [Å] and angles [°] for compounds $[2][\text{BF}_4]$, $[3][\text{BPh}_4]$, and $[4][\text{BPh}_4]$

| | $[2][\text{BF}_4]$ | $[3][\text{BPh}_4]$ | $[4][\text{BPh}_4]$ |
|-------------|--------------------|---------------------|---------------------|
| C15–C22 | 1.403(15) | | |
| C15–Rh1 | 2.091(10) | | |
| C18–C19 | 1.384(14) | | |
| C18–Rh1 | 2.102(10) | | |
| C19–Rh1 | 2.106(9) | | |
| C22–Rh1 | 2.091(10) | | |
| N1–Rh1 | 2.115(7) | 2.081(6) | 2.015(3) |
| N3–Rh1 | 2.513(7) | 2.566(5) | 2.120(2) |
| N4–Rh1 | 2.216(8) | 2.107(5) | 2.022(3) |
| C15–Rh1 | | 1.803(9) | 1.809(4) |
| C16–Rh1 | | 1.800(10) | |
| C6–N3–C9 | 113.4(8) | 111.0(5) | 111.8(2) |
| C6–N3–C7 | 111.2(8) | 109.0(5) | 113.2(2) |
| C9–N3–C7 | 112.2(8) | 114.7(5) | 113.1(2) |
| C6–N3–Rh1 | 99.7(5) | 100.1(4) | 105.3(2) |
| C9–N3–Rh1 | 106.9(6) | 106.7(4) | 103.9(2) |
| C7–N3–Rh1 | 112.8(6) | 114.3(4) | 108.7(2) |
| C15–Rh1–C18 | 82.6(4) | | |
| C15–Rh1–C19 | 97.5(4) | | |
| C22–Rh1–C19 | 81.3(4) | | |
| C15–Rh1–N1 | 92.6(4) | | |
| C22–Rh1–N1 | 92.4(3) | | |
| C18–Rh1–N1 | 166.7(4) | | |
| C19–Rh1–N1 | 154.9(4) | | |
| C15–Rh1–N4 | 173.3(4) | | |
| C22–Rh1–N4 | 143.9(4) | | |
| C18–Rh1–N4 | 102.2(4) | | |
| C19–Rh1–N4 | 89.1(3) | | |
| N1–Rh1–N4 | 81.7(3) | 90.4(2) | 161.9(1) |
| C15–Rh1–N3 | 101.3(4) | | |
| C22–Rh1–N3 | 138.3(4) | | |
| C18–Rh1–N3 | 95.8(3) | | |
| C19–Rh1–N3 | 126.8(3) | | |
| N1–Rh1–N3 | 72.9(3) | 71.7(2) | 81.4(1) |
| N4–Rh1–N3 | 73.8(3) | 72.4(2) | 80.5(1) |
| C15–Rh1–N3 | | 116.9 | 179.3(2) |
| C16–Rh1–N3 | | 115.0(3) | |
| C15–Rh1–N4 | | 89.3(3) | 99.3(1) |
| C15–Rh1–C16 | | 90.0(4) | |
| C16–Rh1–N1 | | 89.3(3) | |
| C15–Rh1–N1 | | | 98.8(1) |



Scheme 1

form and a neutral one $[\text{Rh}(\text{COD})\text{Cl}][\mu, \eta^2-(\mathbf{1})]-[\text{Rh}(\text{COD})\text{Cl}]$.

In order to evaluate the influence of the 1,5-cyclooctadiene on the bonding capabilities of **1**, we replaced the diene by carbon monoxide. Bubbling carbon monoxide into a solution of $[2]^+$ in dichloromethane at room temperature

produces $[\text{Rh}(\text{CO})_2(\mathbf{1})][\text{BF}_4]$ ($[\mathbf{3}][\text{BF}_4]$) which can be isolated as a yellow solid in a nearly quantitative yield. The infrared spectrum in the νCO region shows two strong absorption bands at 2080 and 2011 cm^{-1} , and two weak peaks at 2100 and 2038 cm^{-1} , suggesting the presence of two complexes. This is corroborated by the ^1H NMR spectrum that, analogously to $[\mathbf{2a}]^+$ and $[\mathbf{2b}]^+$, exhibits ethyl resonances for two isomers $[\mathbf{3a}]^+$ and $[\mathbf{3b}]^+$, in the ratio 1:10. However, in contrast to $[\mathbf{2}]^+$, it is the isomer $[\mathbf{3b}]^+$, with the more deshielded ethyl resonances, that is the major compound in solution. For this complex, the methylene protons appear as a broad AB spectrum indicating the existence of a fluxional process in solution. As for $[\mathbf{2}]^+$, the NMR spectroscopic data reveals that there are two isomers where the aminopyrazole ligand can be κ^2 $[\mathbf{3a}]^+$ or κ^3 $[\mathbf{3b}]^+$ bonded. This is corroborated by the infrared data which shows that the minor isomer $[\mathbf{3a}]^+$ exhibits CO absorption at high frequencies, as expected for a 16 valence electron isomer compared to an 18 electron complex. To confirm this hypothesis an X-ray structure determination was undertaken on $[\text{Rh}(\text{CO})_2(\mathbf{1})][\text{BPh}_4]$ ($[\mathbf{3}][\text{BPh}_4]$) obtained by metathesis with NaBPh_4 , which was easier to crystallise than $[\mathbf{3}][\text{BF}_4]$.

Figure 2 depicts cation $[\mathbf{3}]^+$ and salient bond length and angle data are collected in Table 1. The cation has a distorted square pyramid geometry, in which the square plane is defined by the atoms C15, C16, N1, and N4, and the rhodium atom is out of that plane by 0.15 Å. As a consequence of the steric strain imposed by the methylene bridges, the N3 nitrogen atom is not perpendicular to this plane. The Rh–N3 bond is slightly longer than in $[\mathbf{2b}]^+$, but N3 remains within the bonding distance of rhodium. Thus, in the solid state, the structure corresponds to the major isomer $[\mathbf{3b}]^+$ observed in solution. The reduction of the steric crowding around rhodium induced by the replacement of 1,5-cyclooctadiene by two CO molecules is particularly evident if we consider the N1–Rh–N4 angle, which is 81.7(3)° in $[\mathbf{2b}]^+$ and 90.4(2)° in $[\mathbf{3b}]^+$. For the same reasons the Rh–N1 and Rh–N4 bond lengths are, as expected, equal within experimental error.

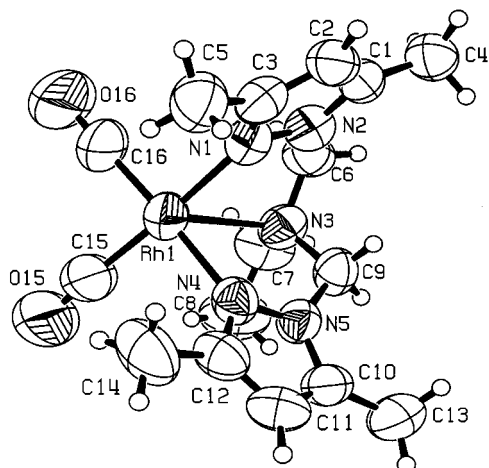
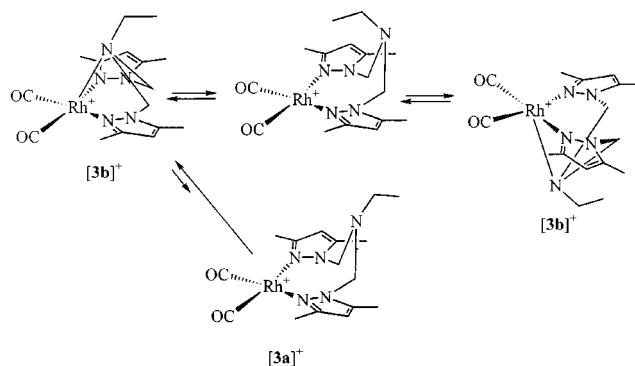


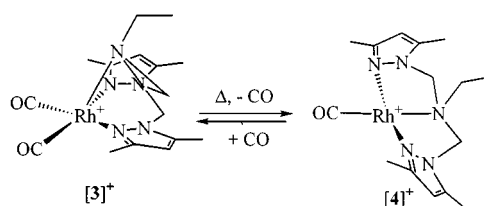
Figure 2. Structure of the cation $[\mathbf{3}]^+$ showing the numbering scheme; ellipsoids are drawn at the 30% probability level

As mentioned above, we observed a broad ^1H NMR AB spectrum for the methylene groups of the isomer $[\mathbf{3b}]^+$, indicating fluxional behaviour in solution for this complex. For this reason we have carried out a variable-temperature ^1H NMR spectroscopic study on the mixture of $[\mathbf{3a}]^+$ and $[\mathbf{3b}]^+$ in $(\text{CD}_3)_2\text{CO}$ solution. For the $[\mathbf{3a}]^+$ spectrum no significant changes were observed during this study. At 253 K the methylene hydrogens of $[\mathbf{3b}]^+$ appear as a narrow AB spectrum, but lowering the temperature to 193 K induces no other significant changes, except for a slight broadening of the *N*-ethyl resonances. Raising the temperature to 333 K brings about coalescence of the AB spectrum to a broad singlet. (The solvent and the thermal stability of the complex did not allow acquisition of spectra above this temperature.) This corresponds to a ΔG^\ddagger value of ca. 70 $\text{kJ}\cdot\text{mol}^{-1}$, a value consistent with the mechanism proposed in Scheme 2 which implies an inversion of configuration of the nitrogen atom.^[18] The initial step is the decooordination of N3, followed by inversion at the nitrogen atom, and subsequent coordination of N3 on the other face of the square plane.



Scheme 2

During the workup of $[\mathbf{3}]^+$, and especially after the evaporation of its solutions under vacuum, we observed the formation, in small quantities, of a new product characterised by a $\nu(\text{CO})$ absorption at 1997 cm^{-1} in the infrared spectrum. This implies a decarbonylation of $[\mathbf{3}]^+$ and, indeed, refluxing a THF solution of $[\mathbf{3}]^+$ induces the nearly quantitative formation of the new complex $[\text{Rh}(\text{CO})(\mathbf{1})][\text{BF}_4]$ ($[\mathbf{4}][\text{BF}_4]$) possessing a $\nu(\text{CO})$ absorption at 1997 cm^{-1} . Bubbling carbon monoxide through a solution of $[\mathbf{4}]^+$ regenerates $[\mathbf{3}]^+$ immediately (Scheme 3).



Scheme 3

The ^1H NMR spectrum of $[\mathbf{4}]^+$ shows only the resonances of the coordinated ligand **1**. The solid-state structure of $[\mathbf{4}]^+$ was established by X-ray crystallography on the tetraphenylborate salt $[\text{Rh}(\text{CO})(\mathbf{1})][\text{BPh}_4]$ ($[\mathbf{4}][\text{BPh}_4]$). A view of $[\mathbf{4}]^+$ is shown in Figure 3 and bond lengths and angles of interest are gathered in Table 1. The cation is square-planar, with the atoms N1, N3, N4, and C15 defining the plane, and the rhodium atom lying 0.02 Å above it. The Rh–N3 bond is longer than the other two Rh–N bonds, a consequence of the *trans* influence of the carbonyl ligand and of the different hybridisation of the nitrogen atom. Owing to the steric strain induced by the methylene bridges, the N1–Rh–N3 and the N3–Rh–N4 angles are less than 90°.

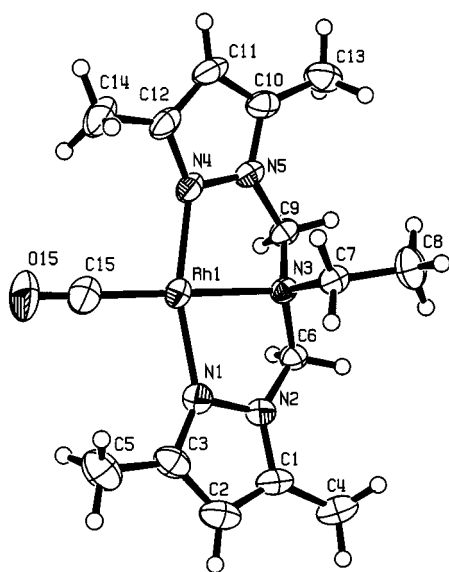


Figure 3. Structure of the cation $[\mathbf{4}]^+$ showing the numbering scheme; ellipsoids are drawn at the 50% probability level

All these structures reveal that **1** is a very flexible ligand that can accommodate, depending on the other ligands around rhodium, either a square-pyramidal geometry in a *fac* configuration or a square planar geometry in a *mer* configuration. Moreover, examination of the structures of other known complexes of bis[(3,5-dimethyl-1-pyrazolyl)methyl]phenyl or ethylamine with Co^{II} ,^[19,20] Ni^{II} ,^[21] Cu^{I} ,^[22] or Cu^{II} ,^[19] salts shows that the most acute $[\mathbf{81.7(3)}^\circ]$ N–M–N angles for the pyrazole ligands have been observed, in our case, with Rh^{I} . The smallest angle observed in the other complexes is 112.5° for the bis[(3,5-dimethyl-1-pyrazolyl)methyl]phenylamine κ^3 bonded to the $\text{Co}(\text{NO}_3)_2$ salt^[20] in a structure intermediate between a distorted trigonal bipyramid and a square pyramid. This shows that, for this family of ligands, the two pyrazolyl groups can equally adopt *cis*-positions in a square plane. In the other extreme of their bonding capabilities, i.e. in a *trans* configuration, 162° seems to be the maximum value these ligands can accommodate: $161.9(1)^\circ$ for the N–M–N angle in $[\mathbf{4}]^+$ and 161.3° in an octahedral complex with the $\text{Ni}(\text{NO}_3)_2$ salt.^[21]

Conclusion

This study provides further evidence of the flexibility of the ligand **1** which adapts its bonding mode to various electronic and steric situations around rhodium(I). For instance, for $[\mathbf{2}]^+$ to compensate the steric bulk of the cyclooctadiene ligand it prefers the κ^2 mode of bonding in solution. In the solid state, it adopts the κ^3 mode of bonding but minimises the steric bulk in the square plane by small variations of the length of the Rh–N (pyrazole) bonds. In the absence of steric strain, it adopts a κ^3 mode of bonding either in a *fac* (complex $[\mathbf{3}]^+$) or a *mer* (complex $[\mathbf{4}]^+$) configuration.

Experimental Section

General Remarks: All reactions were performed under a nitrogen atmosphere with the use of standard Schlenk techniques. Tetrahydrofuran and diethyl ether, used for the synthesis, were distilled under nitrogen from sodium benzophenone ketyl just before use. Other solvents were purified following the standard procedures and stored under nitrogen. – NMR spectra were recorded on Bruker AC 200, AC 250, or AMX 400 instruments. All chemical shift values are given in ppm and are referenced with respect to residual protons in the solvent for proton spectra, to solvent signals for ^{13}C spectra. – Elemental analyses were performed in our laboratory on a Perkin–Elmer 2400 CHN analyser. – The bis[(3,5-dimethyl-1-pyrazolyl)methyl]ethylamine^[9] and $[\text{Rh}(\text{COD})\text{Cl}]_2$ ^[23] have been prepared according to published procedures.

Synthesis of $[\text{Rh}(\text{COD})(\mathbf{1})][\text{BF}_4]$ ($[\mathbf{2}][\text{BF}_4]$): To a solution of 0.079 g (0.16 mmol) of $[\text{Rh}(\text{COD})\text{Cl}]_2$ in 20 mL of THF was added 0.062 g (0.32 mmol) of AgBF_4 and the solution was stirred for half an hour at room temperature. The orange solution turned yellow and AgCl precipitated. The solution was then filtered through a pad of Celite and 0.084 g (0.32 mmol) of **1** was then added. After stirring for an hour, the solution was evaporated to dryness and the residue was crystallised in a dichloromethane/ether mixture to give 0.160 g (90%) of $[\mathbf{2}][\text{BF}_4]$ as yellow crystals. – $\text{C}_{22}\text{H}_{35}\text{BF}_4\text{N}_5\text{Rh}$ (559.3): C 47.24, H 6.32, N 12.52; found C 47.11, H 6.11, N 12.51. Isomer $[\mathbf{2a}]^+$: ^1H NMR (CDCl_3 solution, 250 MHz) δ = 6.58 (d, 2J = 15.4 Hz, 2 H, CH_2N), 5.79 (s, 2 H, CH pyrazole), 5.42 (d, 2J = 15.4 Hz, 2 H, pyrazole CH_2N), 3.99 (b, 4 H, CH cod), 2.76 (q, 3J = 7.1 Hz, 2 H, CH_2CH_3), 2.68 (b, 4 H, CHH_{exo} cod), 2.61 (s, 6 H, CCH_3), 2.56 (b, 4 H, CHH_{endo} cod), 2.25 (s, 6 H, CCH_3), 0.64 (t, 3J = 7.1 Hz, 3 H, CH_2CH_3). – $^{13}\text{C}\{^1\text{H}\}$ NMR (CDCl_3 solution, 50 MHz) δ : 150.8–137.3 (CCH_3), 107.5 (CH pyrazole), 85.2–83.6 (m, =CH cod), 69.4 (CH_2N), 44.8 (CH_2CH_3), 30.8–30.2 (CH_2 cod), 15.6–10.6 (CH_2CH_3 , CCH_3). Isomer $[\mathbf{2b}]^+$: ^1H NMR (CDCl_3 solution, 250 MHz) δ = 5.68 (s, 2 H, CH pyrazole), 4.96 (d, 2J = 12.2 Hz, 2 H, CH_2N), 4.87 (d, 2J = 12.2 Hz, 2 H, CH_2N), 4.14 (q, 3J = 7.2 Hz, 2 H, CH_2CH_3), 3.75 (b, 4 H, =CH cod), 2.68 (b, 4 H, CHH_{exo} cod), 2.60 (s, 6 H, CCH_3), 2.56 (b, 4 H, CHH_{endo} cod), 2.17 (s, 6 H, CCH_3), 1.56 (t, 3J = 7.2 Hz, 3 H, CH_2CH_3). – $^{13}\text{C}\{^1\text{H}\}$ NMR (CDCl_3 solution, 50 MHz) 150.8–137.3 (CCH_3), 107.6 (CH pyrazole), 85.2–83.6 (m, =CH cod), 65.5 (CH_2N), 52.5 (CH_2CH_3), 30.8–30.2 (CH_2 cod), 15.6–10.6 (CH_2CH_3 , CCH_3).

Synthesis of $[\text{Rh}(\text{CO})_2(\mathbf{1})][\text{BF}_4]$ ($[\mathbf{3}][\text{BF}_4]$): Carbon monoxide was bubbled for 1 h through a solution of 0.168 g of $[\mathbf{2}][\text{BF}_4]$ dissolved in 20 mL of dichloromethane. The solution was then evaporated to dryness in vacuum leaving 0.124 g (80%) of **3** as a yellow powder.

– IR (CH₂Cl₂ solution) $\nu(\text{CO})$: 2100 (w), 2080 (s), 2038 (w), 2011 (s) cm^{−1}. Isomer [3a]⁺: ¹H NMR δ = 6.28 (s, 2 H, CH), 5.23 (AB system, ²*J* = 11.7 Hz, 4 H, CH₂N), 3.79 (q, ³*J* = 7.2 Hz, 2 H, CH₂CH₃), 2.64 (s, 6 H, CCH₃), 2.45 (s, 6 H, CCH₃), 1.61 (t, ³*J* = 7.2 Hz, 3 H, CH₂CH₃); Isomer [3b]⁺: ¹H NMR (CD₃)₂CO solution, 250 MHz) δ = 6.29 (s, 2 H, CH), 5.59 (broad AB system, ²*J* = 11.8 Hz, 4 H, CH₂N), 3.16 (q, ³*J* = 7.3 Hz, 2 H, CH₂CH₃), 2.58 (s, 6 H, CCH₃), 2.35 (s, 6 H, CCH₃), 1.17 (t, ³*J* = 7.3 Hz, 3 H, CH₂CH₃). – ¹³C{¹H} NMR (CDCl₃ solution, 63 MHz) δ = 185 (d, ¹*J* = 69.0 Hz, CO), 151.7 (CCH₃), 144.7 (CCH₃), 108.1 (CH), 65.7 (CH₂N), 50.3 (CH₂CH₃), 16.1, 13.9, 11.2 (2 CCH₃ + CH₂CH₃).

Synthesis of [Rh(CO)₂(1)][BPh₄] ([3][BPh₄]): To a solution of 0.135 g (0.32 mmol) of [3][BF₄] in 10 mL of methanol was added 0.110 g (0.32 mmol) of NaBPh₄ and the solution was stirred for 1 h. A yellow precipitate appeared which was filtered and dried under vacuum. It was recrystallised in a dichloromethane/methanol mixture under a CO atmosphere. C₄₀H₄₃BN₅O₂Rh (739.5): C 64.97, H 5.86, N 9.47; found C 64.52, H 6.01, N 9.20.

Synthesis of [Rh(CO)(1)][BF₄] ([4][BF₄]): A solution of 0.12 g of [3][BF₄] in 20 mL of THF was refluxed for 2 h. The solvent was evaporated to dryness in vacuum leaving 0.1 g of a yellow solid. – IR (CH₂Cl₂ solution) $\nu(\text{CO})$: 1997 cm^{−1}. – ¹H NMR (CDCl₃ solution, 200 MHz) δ = 5.95 (s, 2 H, CH), 5.28 (AB system, ²*J* = 12.1 Hz, 4 H, CH₂N), 2.93 (q, ³*J* = 7.4 Hz, 2 H, CH₂CH₃), 2.37 (s, 6 H, CCH₃), 2.18 (s, 6 H, CCH₃), 0.98 (t, ³*J* = 7.4 Hz, 3 H, CH₂CH₃). – ¹³C{¹H} NMR (CDCl₃ solution, 50 MHz) δ = 188.3

(d, ¹*J* = 78.0 Hz, CO), 152.7 (CCH₃), 142.7 (CCH₃), 107.3 (CH), 68.7 (CH₂N), 51.6 (CH₂CH₃), 14.5–11.8, 11 (CH₂CH₃ + 2 CCH₃).

Synthesis of [Rh(CO)(1)][BPh₄] ([4][BPh₄]): To a solution of 0.1 g of [4][BF₄] in 10 mL of methanol was added 0.110 g (0.32 mmol) of NaBPh₄ and the solution was stirred for 1 h. A yellow precipitate appeared which was filtered and dried under vacuum. It was recrystallised in a dichloromethane/methanol mixture. C₃₉H₄₃BN₅ORh (711.5): C 65.82, H 6.10, N 9.84; found C 65.67, H 5.79, N 9.63.

X-ray Crystallographic Study: Crystals of [2][BF₄], [3][BPh₄], and [4][BPh₄] suitable for X-ray diffraction were obtained through recrystallisation from a dichloromethane/ether mixture for [2][BF₄] and dichloromethane/methanol mixture for [3][BPh₄], and [4][BPh₄]. Data were collected on an STOE IPDS diffractometer at 160 K [2][BF₄] and [4][BPh₄], and at 298 K [3][BPh₄]. Full crystallographic data for the three complexes are gathered in Table 2. All calculations were performed on a PC-compatible computer using the WinGX system.^[24] The structures were solved using the SIR92 program,^[25] which revealed in each instance the position of most of the non-hydrogen atoms. All remaining non-hydrogen atoms were located by the usual combination of full-matrix least-squares refinement and difference electron density syntheses by using the SHELXS97 program.^[26] Phenyl ring within the tetraphenylborate counter anion in the structure of [4][BPh₄] have been refined as rigid groups (*D*_{6h} symmetry; C–C = 1.39 Å; C–H = 0.93 Å). Atomic scattering factors were taken from the usual tabulations.^[27] Anomalous dispersion terms for Rh were included in *F*_c.^[28] All non-hydrogen atoms were allowed to vibrate anisotropically. All

Table 2. Crystal data for [2][BF₄], [3][BPh₄], and [4][BPh₄]

| compound | [2][BF ₄] | [3][BPh ₄] | [4][BPh ₄] |
|---|---|---|---|
| empirical formula | C ₆₆ H ₁₀₅ B ₃ F ₁₂ N ₁₅ Rh ₃ | C ₄₁ H ₄₅ BCl ₂ N ₅ O ₂ Rh | C ₃₉ H ₄₃ BN ₅ ORh |
| molecular mass, g | 1677.81 | 824.44 | 711.50 |
| temperature, K | 160(2) | 298(2) | 160(2) |
| wavelength, Å | 0.71073 | | |
| crystal system | triclinic | monoclinic | triclinic |
| space group | <i>P</i> $\bar{1}$ (#2) | <i>P</i> 2 ₁ / <i>c</i> (#14) | <i>P</i> $\bar{1}$ (#2) |
| <i>a</i> , Å | 11.958(2) | 10.562(1) | 10.335(1) |
| <i>b</i> , Å | 15.218(2) | 13.757(1) | 11.549(1) |
| <i>c</i> , Å | 20.010(3) | 28.379(3) | 15.208(2) |
| α , deg | 85.76(2) | | 80.38(1) |
| β , deg | 81.15(2) | 95.93(1) | 87.04(1) |
| γ , deg | 88.24(2) | | 84.89(1) |
| volume, Å ³ | 3587.3(8) | 4101.6(7) | 1781.3(3) |
| <i>Z</i> | 2 | 4 | 2 |
| <i>D</i> _{calcd.} , g·cm ^{−3} | 1.553 | 1.335 | 1.327 |
| μ , mm ^{−1} | 0.765 | 0.587 | 0.517 |
| <i>F</i> (000) | 1728 | 1704 | 740 |
| θ range, deg | 2.07–25.99 | 2.07–26.23 | 2.56–26.16 |
| index ranges | −14 ≤ <i>h</i> ≤ 14 −18 ≤ <i>k</i> ≤ 18 −24 ≤ <i>l</i> ≤ 24 | −12 ≤ <i>h</i> ≤ 13 −16 ≤ <i>k</i> ≤ 16 −34 ≤ <i>l</i> ≤ 35 | −12 ≤ <i>h</i> ≤ 12 −14 ≤ <i>k</i> ≤ 14 −18 ≤ <i>l</i> ≤ 18 |
| reflections collected | 35478 | 28064 | 17761 |
| independent reflections | 13042 [<i>R</i> (int) = 0.0332] | 7859 [<i>R</i> (int) = 0.0791] | 6528 [<i>R</i> (int) = 0.0286] |
| completeness to θ_{max} , % | 92.5 | 95.2 | 90.9 |
| refinement method | full-matrix least-squares on <i>F</i> ² | | |
| data/restraints/parameters | 13042/0/902 | 7859/0/474 | 6479/0/491 |
| g.o.f. on <i>F</i> ² | 0.823 | 0.856 | 1.043 |
| <i>R</i> [<i>I</i> > 2σ(<i>I</i>)] | 0.0251 | 0.0577 | 0.0404 |
| <i>R</i> [<i>I</i> > 2σ(<i>I</i>)] | 0.0687 | 0.1475 | 0.1012 |
| <i>R</i> (all data) | 0.0895 | 0.1529 | 0.0466 |
| <i>R</i> (all data) | 0.0909 | 0.2072 | 0.1052 |
| residual electron density e [−] ·Å ^{−3} | 0.424 and −0.501 | 0.373 and −0.622 e | 0.836 and −0.654 |

the hydrogen atoms were set in an idealised position (R_3CH , $C-H = 0.96 \text{ \AA}$; $R_2CH_2 = 0.97 \text{ \AA}$; $C(sp^2)-H = 0.93 \text{ \AA}$; U_{iso} 1.2 times greater than the U_{eq} of the carbon atom to which the hydrogen atom is attached) and held fixed during refinements. Crystallographic data (excluding structure factors) for the structures reported in this paper have been deposited with the Cambridge Crystallographic Data Centre as supplementary publication n° CCDC 16295, CCDC 16296, CCDC 16297. Copies of the data can be obtained free of charge on application to CCDC, 12 Union Road, Cambridge CB2 1EZ, UK; Fax: (internat.) +44-1223/336-033; E-mail: deposit@ccdc.cam.ac.uk.

Acknowledgments

We thank Professor Michael J. McGlinchey for improving the manuscript and for fruitful discussions. Support by the CNRS and the Ministerio de Educacion y Cultura of Spain (Projects PB96-1146 and BQU200-0238 and grant to G. E.) are gratefully acknowledged.

- [1] S. Trofimenko, *Scorpionates: The coordination chemistry of polypyrazolylborate ligands*. Imperial College Press, London, **1999**.
- [2] S. Trofimenko, *Prog. Inorg. Chem.* **1986**, *34*, 115–210.
- [3] P. K. Byers, A. J. Canty, R. T. Honeyman, *Adv. Organomet. Chem.* **1992**, *34*, 1–65.
- [4] R. Mukherjee, *Coord. Chem. Rev.* **2000**, *203*, 151–218.
- [5] N. Kitajima, W. B. Tolman, *Prog. Inorg. Chem.* **1995**, *43*, 419–531.
- [6] M. Etienne, *Coord. Chem. Rev.* **1996**, *156*, 201–236.
- [7] G. Parkin, *Adv. Inorg. Chem.* **1995**, *42*, 291–393.
- [8] G. Parkin, *Chem. Commun.* **2000**, 1971–1985.
- [9] W. L. Driessen, *Recl. Trav. Chim. Pays-Bas* **1982**, *101*, 441.
- [10] H. L. Blonk, W. L. Driessen, J. Reedijk, *J. Chem. Soc., Dalton Trans.* **1985**, 1699–1705.
- [11] [11a] A. Togni, L. M. Venanzi, *Angew. Chem.* **1994**, *106*, 517ff.; *Angew. Chem. Int. Ed. Engl.* **1994**, *31*, 497–526. [11b] F. Fache, E. Schulz, M. Lorraine Tommasino, M. Lemaire, *Chem. Rev.* **2000**, *100*, 2159–2231.
- [12] T. Ohkuma, D. Ishii, H. Takeno, R. Noyori, *J. Am. Chem. Soc.* **2000**, *122*, 6510–6511.
- [13] K. Abdur-Rashid, A. J. Lough, R. H. Morris, *Organometallics* **2000**, *19*, 2655–2657.
- [14] M. Akita, M. Hashimoto, S. Hikichi, Y. Moro-oka, *Organometallics* **2000**, *19*, 3744–3747 and references therein.
- [15] D. Sanz, M. D. Santa Maria, R. M. Claramunt, M. Cano, J. V. Heras, J. A. Campo, F. A. Ruiz, E. Pinilla, A. Monge, *J. Organomet. Chem.* **1996**, *526*, 341–350.
- [16] See for instance: M. Akita, K. Ohta, Y. Takahashi, S. Hikichi, Y. Moro-oka, *Organometallics* **1997**, *16*, 4121–4128.
- [17] G. Esquiús, J. Pons, R. Yáñez, J. Ros, *J. Organomet. Chem.* **2001**, *619*, 14–23.
- [18] H. Günther, *NMR Spectroscopy*, John Wiley & Sons, **1980**.
- [19] H. L. Blonk, W. L. Driessen, J. Reedijk, *J. Chem. Soc., Dalton Trans.* **1985**, 1699–1705.
- [20] K. Locher, H. L. Blonk, W. L. Driessen, J. Reedijk, *Acta Crystallogr., Sect. C* **1987**, *43*, 651–653.
- [21] J. W. F. M. Schoonhoven, W. L. Driessen, J. Reedijk, G. C. Verschoor, *J. Chem. Soc., Dalton Trans.* **1984**, 1053–1058.
- [22] Y. C. M. Pennings, W. L. Driessen, J. Reedijk, *Acta Crystallogr., Sect. C* **1988**, *44*, 2095–2097.
- [23] G. Giordano, R. H. Crabtree, *Inorg. Synthesis* **1990**, *28*, 88–90.
- [24] L. J. Farrugia, *J. Appl. Crystallogr.* **1999**, *32*, 837.
- [25] A. Altomare, G. Cascarano, C. Giacovazzo, A. Guagliardi, *J. Appl. Crystallogr.* **1993**, *26*, 343.
- [26] G. M. Sheldrick, *SHELXS97, SHELXL97, CIFTAB – Programs for Crystal Structure Analysis (Release 97–2)*, Institut für Anorganische Chemie der Universität, Tammanstraße 4, 3400 Göttingen, Germany (**1998**).
- [27] [27a] D. T. Cromer, J. T. Waber, *International Tables for X-ray Crystallography*; Kynoch Press: Birmingham, England, vol. 4, **1974**, Table 22B. – [27b] R. F. Stewart, E. R. Davidson, W. T. Simpson, *J. Chem. Phys.* **1965**, *42*, 3175. – [27c] T. Hahn, Ed., *International Tables for Crystallography, Volume A*, Kluwer Academic Publishers, Dordrecht, The Netherlands (**1995**).
- [28] D. T. Cromer, J. T. Waber, *International Tables for X-ray Crystallography*, Kynoch Press: Birmingham, England, vol. 4, **1975**, Table 2.3.1.

Received April 6, 2001
[I01124]